

Switchable RF over Fiber for Low-Cost Operation of Many RF Inputs

Justin Gruber, Francisco Hernandez, James Ko, Edgar Nino

Dept. of Electrical Engineering and Computer Science, University of Central Florida, Orlando, Florida, 32816-2450

Center for Research and Education in Optics and Lasers (CREOL), University of Central Florida, Orlando, Florida, 32816-2450

ABSTRACT — We demonstrate a radio over fiber (RoF) system that has an asymmetric design in which three RF sources are transmitted using only two wavelengths of light. To enable this, we utilize MEMS fiber switches in order to selectively direct each laser to one of three modulators. Each of these modulators is connected to one of the three RF sources, in effect allowing each laser to be selectively modulated with one of three RF signals. This reduces the amount of optical hardware needed in the system. This system could be scaled to larger numbers of RF sources, and at larger RF sources the savings on optical hardware grow more pronounced.

Index Terms — RF, fiber-optics

I. INTRODUCTION

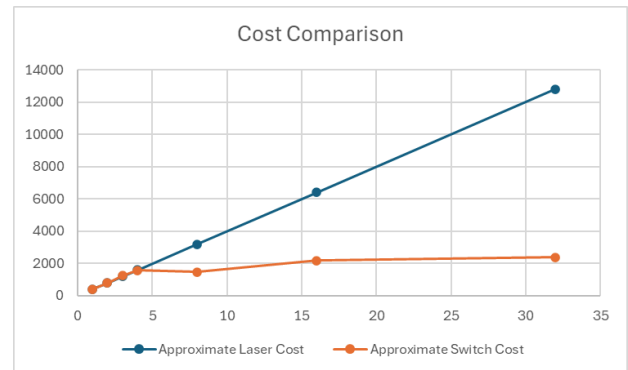
Radio over fiber has become a widespread and mature technology for the transmission of RF signals. Rather than using traditional coaxial cables to send electrical RF signals, a RoF system does this by encoding the RF signal in the intensity of light traveling through a fiber optic cable. This has benefits in improving the bandwidth of an RF system and has orders of magnitude of lower losses, especially at high frequencies.

A typical Radio-over-Fiber (ROF) system relies on several interconnected subsystems to achieve signal transmission, reception, and detection. This includes an antenna or another RF source to generate the initial signal to be transmitted, RF processing components such as filters, Digital-to-Analog Converters (DACs), and amplifiers to process the signal, a laser to act as the carrier, a modulator to encode the RF signal in the intensity of the laser light, low loss optical fiber to carry the light over long distances, and a photodiode to recover the electrical signal from the light intensity.

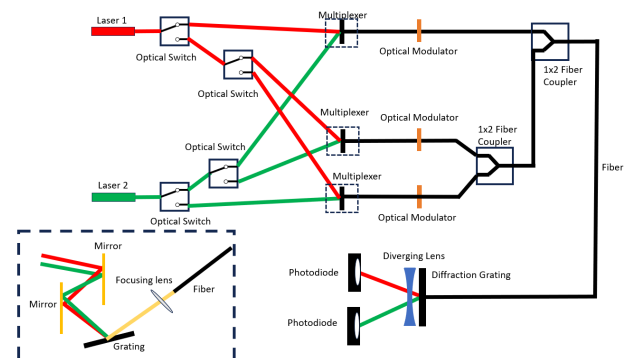
Traditional RoF setups employ a one-to-one architecture. This means that when transmitting data from multiple RF sources, each source requires a dedicated laser source and photodiode. This design becomes inherently inefficient if only a subset of the RF sources is active at

any given time, failing to utilize the full capacity of the link. To remedy this problem, we designed a system with fiber optic switches and a wavelength division multiplexing (WDM) system. This system allows for real-time switching of the RF source being transmitted to any of the photodiodes. In addition, this switching is nonblocking, meaning a single antenna can have its RF signal sent to multiple receivers.

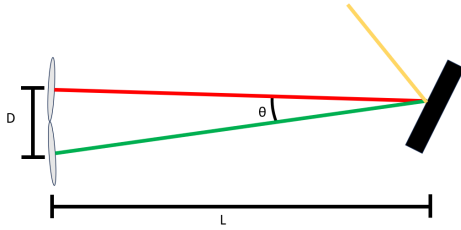
This unique capability can be used to construct an asymmetrical system in which there are more RF sources (antennas) than there are receivers (photodiodes). In this project, we demonstrate a system with three RF sources and two photodiodes to show a proof of concept of this asymmetrical switch-based architecture. These three RF sources will operate at three different frequency ranges. Thus, we can cover three different frequency ranges with only two photodiodes. While this proof-of-concept system only adds one additional RF source, we provide analysis to show that this concept is scalable to larger numbers of RF sources.



This technique offers distinct advantages over a single wideband antenna. Wideband antennas, while offering a broader bandwidth, often come with trade-offs in other areas. These trade-offs can include lower sensitivity, a lower Q-factor, and higher noise figures. For this reason, our design provides a unique solution to covering a large range of RF frequencies while providing high-quality RF transmission and detection while minimizing the amount of expensive optical hardware needed.



To develop this project, we need to design and integrate several subsystems. The first is the RF subsystem, responsible for generating, filtering, and amplifying the signals. The second is the optical subsystem, which generates the light carrier and modulates the RF signal onto it. Laser diodes and Mach-Zehnder interferometers are key components for achieving this modulation. The third subsystem utilizes electronically controlled 1x2



fiber optic switches to direct an input fiber's signal to one of two output fibers. A diffraction grating is then used to combine the various wavelengths of light, which are then coupled into a single fiber for transmission. At the receiver end, we again used a diffraction grating for demultiplexing and then photodiodes to recover the RF signal from the light intensity. Along with this hardware we require a software system to enable control over the switching mechanism, allowing the user to easily choose which RF sources are active.

II. Wavelength Division Multiplexing

A. Diffraction Grating

Wavelength division multiplexing is the use of several distinct wavelengths in a communications link, each of which is independently modulated. This allows for each wavelength to carry a unique signal, increasing the bandwidth of the channel by the number of wavelengths used. This necessitates the use of an optical element that has either diffractive or dispersive properties to selectively direct the different wavelength channels. When this effect is used to combine several wavelengths into a single channel, it is known as multiplexing. The reverse, in which several wavelengths in a single channel are separated, is known as demultiplexing.

In our project, we require the ability to multiplex the several signals together into a fiber for transmission, and then demultiplex the signals to be read out. For multiplexing, the two wavelengths are incident upon a diffraction grating at different angles chosen such that the two beams are diffracted at the same angle. This allows the two beams to be collinear, and couple into the same fiber. In order to calculate the necessary angle between the two beams, we must take into account the wavelengths of light being used as well as the geometry of the diffraction grating. The diffraction grating geometry is defined by the lines per mm of the grating,

and based on this and the center frequency the blaze angle can be found. This blaze angle is the angle at which the diffraction grating will have the highest efficiency. For this reason, we operate our 1550 nm laser at the blaze angle of the grating. For our diffraction grating, the design wavelength is 1550 nm and the corresponding blaze angle is found according to the equation

$$2a * \sin(\theta_L) = m\lambda \quad (1)$$

where a is the grating spacing and m is the order of the diffracted beam. Solving this equation gives a blaze angle of 68.4348 degrees. We then use the diffraction grating equation

$$a[\sin(\theta_M) + \sin(\theta_i)] = m\lambda \quad (2)$$

To calculate the necessary incident angle at 1530nm. This incident angle must match the condition that the value of θ_M is the same at both 1530 and 1550 nm. For 1550 nm, we have the special case of $\theta_i = \theta_M = \theta_L = 68.4348$ degrees. Thus, we must solve equation 2 for $\theta_M = 68.4348$ degrees and $\lambda = 1530$ nm, which gives the solution of $\theta_i = 64.9583$ degrees.

These two angles have a difference of only 3.476 degrees, which is the angle they must be separated by when converging onto the diffraction grating. To allow for precise alignment of the lasers, they will be mounted on KM05 kinematic mounts. Due to the size of these mounts, the minimum distance between the centers of the two beams is 18 mm. As such, the distance required for the lasers to converge at an angle of 3.476 degrees is given by equation 3.

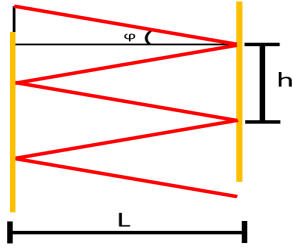
$$\tan(3.476^\circ) = \frac{18\text{mm}}{L} \quad (3)$$

This gives a distance of 29.64 cm, which would result in a large device size.

Figure 1. Geometry of angular separation of beams onto diffraction grating

B. Mirror Cavity

To remedy the large device size, we will use a mirror cavity to achieve the necessary path length in a small physical device. This mirror cavity will consist of two mirrors. The mirrors are aligned parallel to one another and separated by a distance, d . Additionally, there is a lateral offset of 5mm between the mirrors allowing the beams to enter and exit the cavity.



To design the cavity, we must consider the number of roundtrips in the cavity. More round trips shorten the distance between the mirrors, but at the cost of higher losses. The vertical distance traveled in a roundtrip, h , must also be greater than the size of the beam to allow the beam to exit the bottom of the cavity without clipping. We can relate L , h , and the angle ϕ according to the equation $\tan(\phi)=h/2L$. In order to have a small device, we wish to have $L = 5\text{cm}$. We then require that $2*h > 20\text{mm}$ for the beam to exit the cavity. Additionally, we require $1.5*h < 23\text{mm}$ such that the last reflection from the right mirror does not clip off the mirror. As result, we see that $15.33 > h > 10$. Due to physical constraints in the mounting of the hardware, the value of $h = 13.5 \text{ mm}$ was chosen. From this value and the length of the cavity, we then calculate the necessary angle using equation 4.

$$\tan(\phi) = \frac{h/2}{L} \quad (4)$$

From this we see that $\phi = 7.688^\circ$.

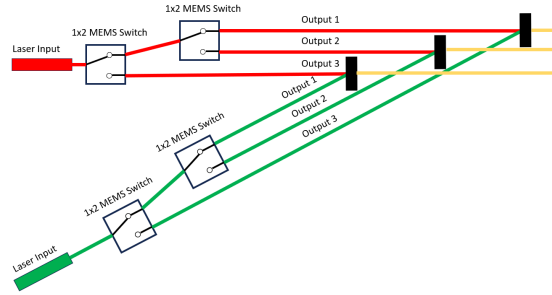
The angle ϕ will be in the horizontal plane, while the angle difference θ is in the vertical direction. At the output of the mirror cavity, the two beams will intersect with each other and be incident upon the diffraction grating.

III. Fiber Optic Switching

The switching of optical signals between different paths is a fundamental part of our project. This switching allows for 2 wavelengths to be able to transmit information from 3 different RF front ends. This reduces the amount of optical hardware needed to serve the 3 RF systems. Of course, this means that not all of the RF systems can be utilized at once. However, this has potential benefits in applications in which access to a wide range of different RF frequencies is desired, but simultaneous access to all bands is not needed.

The switching mechanism of our project will be performed by MEMS-based fiber switches. Although this is a mechanical switch, the MEMS switch is highly reliable with a lifespan of billions of cycles. This property along with low losses make MEMS switches ideal for our project.

To create these 1x3 switches, we will cascade two 1x2 switches, with the input of the second being one of the outputs of the first. This allows us to have a single input and three output states. The two 1x3 switches will then be combined using three of the multiplexing setups. Each multiplexing setup's output is then connected to one of the three



modulators.

This allows for either wavelength to be directed into any of the three RF systems. After the two signals are multiplexed at each of the three modulators, the modulator outputs are combined using 2x1 fiber couplers. This results in the output from all three modulators being combined into a single fiber for transmission.

Figure 4. Design of 2x3 multiplexing system

IV. Demultiplexing

The demultiplexing system operates in the same manner as the multiplexing system, but with the direction of the light beams reversed. Now, the combined beam consisting of 1550 and 1530 nm light will be incident upon the diffraction grating. The two beams are then diffracted with an angular difference equal to the angle found in the multiplexing system. The mirror cavity has the same geometry, except now the direction of light travel is reversed. The spatial separation of the two beams increases as it travels through the mirror cavity, until it matches the separation of the photodiodes. At this point, the light is incident upon the two photodiodes, enabling the two signals to be detected.

V. Polarization Control

Several elements of our system are highly sensitive to the polarization of light. For this reason, we require the ability to control the polarization of light propagating in our fibers. However, most of the components are coupled to single mode fiber, and not polarization-maintaining fibers. For this reason, we designed and constructed fiber polarization controllers that enable the tuning of the polarization direction of light in the system.

These fiber polarization controllers are necessary prior to the modulators and diffraction gratings, as each of these components are designed for a specific polarization with respect to the device. If the polarization is not correct,

these devices will have significantly increased losses. The basic principle on which these polarization controllers operate is stress-induced birefringence. When a fiber is looped in a circular pattern, a birefringence is induced by the radial stress induced on the fiber in the plane of the loops. The fast axis is in the plane of the spool, and the slow axis is perpendicular to the plane of the spool. The total retardance of the spool is determined by the geometry of the fiber as well as the number of loops and diameter of the spool. Through this method, we create two spools with retardation of a half and quarter wave. By varying the relative angle between these two spools, we can rotate the polarization direction of the linearly polarized light.

$$\phi = \frac{\pi n \Delta d^2}{\lambda D} \quad (5)$$

For this project, we plan to use a two-paddle fiber polarization controller. The first paddle is designed to act as a half-wave plate, and the second plate as a quarter-wave plate. This similarity to a set of free space waveplates allows us to model its behavior using Jones matrices, as shown in Equation (6).

$$\begin{bmatrix} E_{x,out} \\ E_{y,out} \end{bmatrix} = \underbrace{\begin{bmatrix} 1 & 0 \\ 0 & 0 \end{bmatrix}}_{\text{vertical polarizer}} * \underbrace{\left(\frac{1}{\sqrt{2}} \begin{bmatrix} 1 - j \cos(2\theta_2) & -j \sin(2\theta_2) \\ -j \sin(2\theta_2) & 1 + j \cos(2\theta_2) \end{bmatrix} \right)}_{\text{Quarter wave plate}} * \underbrace{\left(-j \begin{bmatrix} \cos(2\theta_1) & \sin(2\theta_1) \\ \sin(2\theta_1) & -\cos(2\theta_1) \end{bmatrix} \right)}_{\text{Half wave plate}} \begin{bmatrix} E_{x,in} \\ E_{y,in} \end{bmatrix} \quad (6)$$

Ideally, our laser light should maintain a linear polarization state as it propagates through the fiber. However, due to polarization mode dispersion (PMD) in single-mode fibers, different polarization components travel at slightly different speeds. This effect can cause the initially linear polarization of the laser light to become circular or elliptical after propagating through at least 2 meters of fiber, or after a disturbance like shaking the fiber.

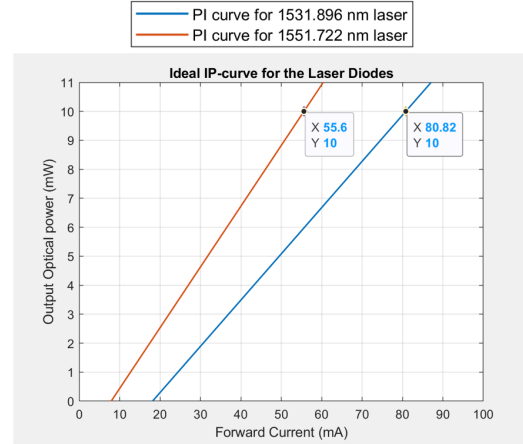
For the case in which linear polarized light becomes elliptically polarized, we can use a half-wave plate to rotate the major axis of the ellipse to 45 degrees relative to the quarter-wave plate's (QWP) fast axis. The phase shift introduced by the QWP can then convert it back to linearly polarized light at a certain orientation angle with respect to the horizontal axis. If the linearly polarized light becomes circular, we can orient the half-wave plate to 0 or 90 degrees, leaving the polarization state unaffected. However, upon reaching the QWP, circular light will be transformed into linearly polarized light at a 45-degree angle, depending on whether it's left- or right-handed circular polarization. The vertical polarizer matrix element in Equation (X) models the Mach-Zehnder modulator's polarization-sensitivity. For simplicity, we can assume the modulator acts as a vertical polarizer when the laser light enters, thus allowing us to potentially code the jones matrices into

MATLAB or Desmos, and plot to see the change in behavior with the polarization.

VI. Laser Subsystem

Our project utilizes two distinct 14-pin butterfly-packaged laser diodes as light sources. One laser diode generates a wavelength of 1532nm, while the other generates a wavelength of 1552nm. In fiber optic communication systems, maximizing the laser source's optical output power is ideal for data signals to travel longer distances through the fiber before requiring amplification to regenerate the weakened signal.

Our specific lasers boast a maximum output power of 10 mW. To achieve this level of power, we need to understand the relationship between the optical output power and the forward electrical current, also known as the PI curve. This curve illustrates how the output power changes as a function of the current flowing through the diode. Below a threshold current (I_{th}), the output power is near zero, typically just a few nanowatts (nW). However, exceeding the threshold current leads to a significant and rapid increase in the output power. Beyond this threshold, the power increases proportionally with the current, representing the ideal operating region for efficient and linear operation. Which is what we desire to operate our lasers.



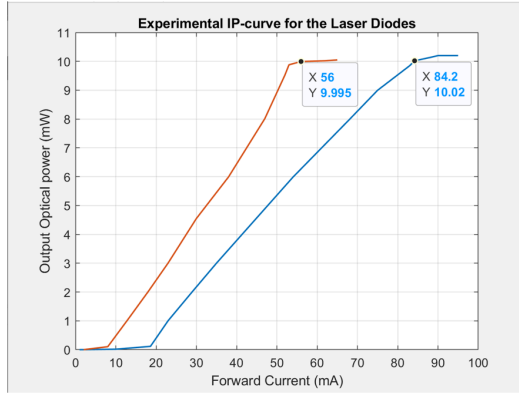


Figure5a & 5b. Ideal and Experimental IP curves for the design of PCB Drivers for the Laser Diodes

The slope efficiency is given by the derivative dP/dI , which is generally constant for the P-I curve in the linear region. Slope efficiency, in the context of a laser diode, refers to the effectiveness of converting electrical current (pump power) into usable optical output power. It's a crucial parameter for characterizing laser performance. Using this efficiency, the output power due to stimulated emission, can be determined by the following expression for any operating current I :

$$P = \frac{dP}{dI} (I - I_{th}) \quad (6)$$

The datasheets for our lasers only provided threshold currents and slope efficiencies. This lack of information on test currents for achieving specific optical powers necessitated the derivation of the equations for their PI curves. The 1550nm laser has a threshold current of 18.16 mA and a slope efficiency of 0.1596 mW/mA. Similarly, the 1530nm laser exhibits a threshold current of 7.929 mA and a slope efficiency of 0.2097 mW/mA. Figure X(a) shows the ideal PI curves for both lasers. These curves indicate the forward currents needed to achieve 10 mW of optical power: 55.6 mA for the 1550nm laser and 80.82 mA for the 1530nm laser. It's important to note that ideal PI curves don't exhibit limitations like saturation. Figure X(b) presents the experimental PI curves obtained by testing the lasers with their driving PCBs. This data reveals the important characteristic of optical power saturation in the lasers, meaning they cannot exceed a certain power output (around 10 mW in this case) even with increased current. Additionally, butterfly-packaged lasers like these typically incorporate a built-in thermoelectric cooler (TEC) module for improved performance. High temperatures degrade the laser over time and can also shift its wavelength depending on the package temperature. The TEC module requires a driving current of around 0.6 A, which the PCB is designed to provide alongside the current for the laser diodes.

VII. RF and Optical Modulator Subsystem

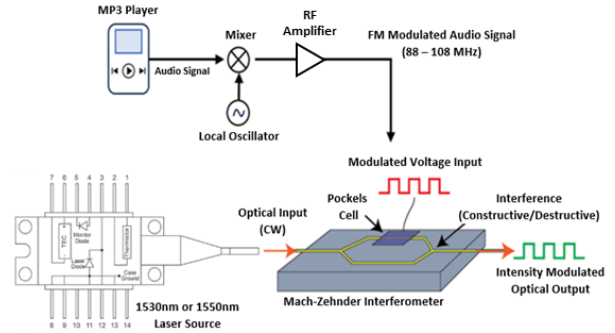
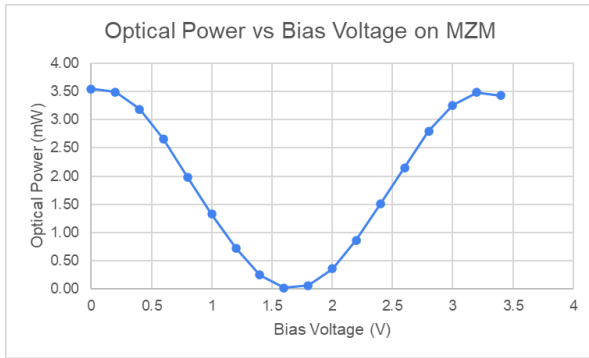


Figure 7. Schematic of RF and optical modulator subsystems For the radio frequency (RF) bandwidth requirements of the RoF subsystem, we aim to transmit signals within the range of 30 MHz to 5 GHz. This wide bandwidth opens doors to various applications, including 5G fronthaul, CATV and internet access, microwave backhaul, radar, and radio astronomy. To achieve this, two key components are necessary: a Mach-Zehnder interferometer and RF amplifiers with bandwidths that match the system's requirements. We have selected the 3157-ZX60-V63+ Low Noise Amplifier (LNA) from Mini-Circuits as our RF amplifier. This LNA boasts a bandwidth ranging from 50 MHz to 6 GHz, exceeding our system's needs. For the Mach-Zehnder interferometer, we will be using the T.MXH1.5-40PD-ADC-LV model from Sumitomo Osaka Cement Co. This interferometer offers an impressive bandwidth from 0 to 20 GHz, significantly exceeding the system's required range.

Ideally, with these two components, we can effortlessly transmit any RF frequency within our desired bandwidth (30 MHz to 5 GHz). However, finding a readily available RF source that directly generates high RF frequencies proved challenging. This hurdle can be overcome by utilizing a low-frequency source (in the kHz range) and cascading a mixer and voltage-controlled oscillator (VCO) to upconvert the signal to the target range. For our final demo, we will employ this up-conversion technique. We plan to connect an MP3 player or ESP32 to a mixer and a local oscillator with a bandwidth of 78 to 108 MHz. This setup will allow us to frequency modulate the audio signal, as shown in Figure 7. To transmit higher frequencies within the sub-GHz to GHz range, we will utilize the Rohde & Schwarz SMA100A Signal Generator. This instrument offers the capability to transmit sine and square wave signals across a broad range, from 9 kHz to 3 GHz.

To transmit the RF signal into an optical fiber, we must encode the RF signals into the intensity of the laser light. The Mach-Zehnder interferometer can do so long as the

amplitude of the RF signal is greater than the pi voltage of interferometer, which is 1.6V. This is doable as our RF amplifier can amplify the signal up to an amplitude of approximately 5V. The pi voltage ($V\pi$) represents the voltage difference required between the two arms of the Mach-Zehnder interferometer to induce a π -radians phase shift between the light paths. This phase shift results in minimal light intensity at the output. Half of the pi voltage ($V\pi/2$) typically corresponds to a point of maximum light intensity output. Our goal is to bias the Mach-Zehnder interferometer at $V\pi/2$. We experimentally found $V\pi/2$ to be approximately 3.3V as shown in figure 8. However, because the modulator we bought has an insertion loss of 4.5 dB due to coupling a fiber to a waveguide, instead of expecting an optical output of 10mW similar to our input we end up with at most 3.55 mW of optical power. In addition, equation 7, shown below, analytically describes the relationship between the optical output power and the bias voltage of the Mach-Zehnder interferometer.



$$P_{out,MZM} = 0.5 * IL * P_{in} \left[1 + \cos\left(\frac{\pi * V_{input}}{V_{\pi}}\right) \right]$$

$$= 1.775 \left[1 + \cos\left(\frac{\pi * V_{input}}{1.6V}\right) \right]$$

Figure 8. Transfer Function of the Mach Zehnder Modulator

VIII. Hardware Components

The system needs several components to have a control unit for the switch drivers and generate analog signals for optical modulation. The chosen components for this task are two MCUs, and their required electronics components such as a crystal oscillator to provide a reference signal for timing operations, decoupling capacitors to guarantee a stable power supply even in case of a power fluctuation, and some resistors to bias internal components.

It is worth noticing that the electronic hardware for the electronic system is split into several PCBs for the sake of simplicity and to make them easier to integrate because the outputs and input signals from the PCB to

the optical system are needed in two spaces that are separated by a considerable distance. Thus, splitting the electrical system provides the required flexibility for that constraint, and it is easier to design and debug two different PCBs with half of the number of components for each since there will not be as many traces, which also increases the chances of using a two-layer PCB (signal and ground), instead of implementing a four-layer PCB which would increase the chances of error and also may imply complex debugging, and testing if there is a mistake in the inner layouts of it.

A. MSP430G2553

This microcontroller is used to create a combination for the MEM switches to multiplex the optical transmission through the optic fiber. The simplicity, low power consumption, ease of integration, and familiarity with this MCU led us to choose it over any other option.

B. ESP - WROOM - 32

This Microcontroller is responsible for the wireless communication front end, that is, receiving, filtering, amplification, modulation, and demodulation of a signal. This component will receive a wireless signal and then output the embedded data as an analog signal that will be used for multiplexing.

C. Logic Shifter

In order to make the MEMS switches work, it is necessary to use switch drivers that require 4 to 4.2 volts to actuate the switches. However, the output voltage of the MSP430 is 3.3V, which makes it necessary to add extra circuitry to output the needed 4 Volts to actuate the switches. This circuit is called a Logic shifter, and what it does is take two voltage level inputs, and outputs one of them depending on if it will shift the voltage to a higher or lower level.

To realize a logic shifter circuit, it is req_i (7) use a device that can control whether current flows or not, and a transistor is used for that purpose. In this case, an n-channel MOSFET is used as the current flow-controlling device. The transistor's configuration is the next one. The 3.3 volts are applied to the Gate, and there is a resistor between the gate and the Drain nodes. The Drain is connected to a parallel connection, one to a resistor that performs a voltage division when the transistor is on, and to a pin of the MSP430 and it can be modeled as a 12 Mega Ohm resistor. The equivalent resistance of these two resistors in parallel, when the MOSFET is conducting, is just the resistor with a small value (when compared to the Source resistor)

Finally, the Source is connected to the 5volts voltage source through a series resistor and to the input of the switch driver. Therefore, when the output voltage of the pin of the MSP430 is on (3.3V), the MOSFET is not conducting because the voltage drop from the Gate to the

Drain is zero, which in consequence, makes the voltage output of it 5 Volts to the switch driver. Furthermore, the value of the resistors must be chosen with respect to each other except for the 2k Ohm resistor. With the intention of having an output that does not activate the switch, a voltage division is done with the Source and Drain resistor so that most of the voltage is dropped in the last one.

X. SOFTWARE COMPONENTS

In the project, we implemented a three-part system. In the above figure, shows the state diagram of the MCUs. One that will control the analog to digital conversion and the encryption of signals being sent out. Another that will deal with the switches for the RF. The last one will oversee receiving and decrypting the signals it receives.

The first and last components here are the same kind of MCU, however they will be doing the opposite duties. The language chosen to code these MCU is in C++. We found this easier to implement than regular C. The MCU that was chosen was the ESP32. It is capable of Bluetooth and Wi-Fi connections, so it was the best decision to implement into this project as we would need to go back and forth from analog to digital and back from digital to analog to showcase the intent of this project.

A. Sending signal

The program for this code starts by initializing every component and giving the part a quick test to ensure functionality. Along with starting the system to engage with analog signals. When a signal is then ready to be sent the operator of the system will press a button(s) in a binary format to direct the optics to the desired destination. These button presses will flip the necessary switches to get the laser to the right end point. While the operator is adjusting the end point for the signal, the MCU will go ahead and start using the analog to digital converter to make the signal capable of optic transfer. After which the now digitized signal will also be encrypted in the Advanced Encryption Standard encryption scheme to ensure the safety of the signal being sent.

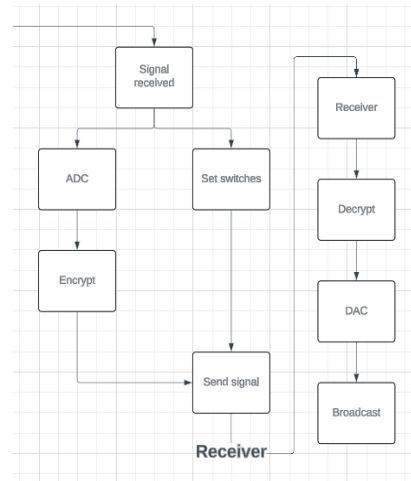


Figure 10. ESP32 and MSP430 coding state diagram

The signal is now ready to be delivered as it is sent through the optics with the two other MCU's ready to receive the signal. One will have the encryption key necessary to decrypt the message back to its original form. While the other one will have a random key that will decipher the message but will not get it back to its original form. This second MCU is supposed to represent the "hacking" of messages through unsecure servers that has happened in the past. Both these MCU's will then perform the same sequence of events once receiving the signal. It will firstly use the key in hand to decrypt the message. This message will then be sent to the inner digital to analog converter. This will transcribe this digital signal back to the RF signal it started as and should then produce the same original message.

B. Receiver

The signal is then received by the other MCU. That MCU will store the signal in a temporary variable as it checks the length of that variable so it can create a buffer variable for the decryption. The MCU will use the same shared encryption key to decrypt the message. That message now needs to be converted back into an analog signal so it will be fed through a digital to analog converter. The signal now transferred through optics should be an exact copy of the original image.

C. Encryption

Encryption is a fundamental method of securing sensitive information by formatting the signal or message into an unreadable format. This is done through an encryption algorithm and an encryption key. The algorithm will function based on the key used to activate it. Once based through the algorithm will turn into an unrecognizable string of characters and symbols. The only way to gain access to the original message is to have the same encryption key. Access to the same encryption key will allow the user to decrypt the message

back to an understandable form. Decryption essentially performs the encryption used on it in reverse. Encryption plays a major role in safeguarding data during transmission. The encryption process is used with the ESP32 will start encrypting the message once it has fully converted the signal into a digital signal. Though first it will want to check for the length of the message that was just sent in and will create a buffer to store the new encrypted message. That signal will then be encrypted in the Advanced Encryption Standard scheme. It will then be stored in the buffer until that message is completely encrypted. Then it will be sent through the optics to be received by the other MCUs. One is label “Receiver” and the other as “Hacker”. Both will go through the same process though. It will essentially mirror how the sender did it. First, it will confirm the message received. Then it will create a buffer for the decrypted message. The decryption method works in reverse of how the encryption method did it. Thus, why the changing of the encryption key is shown dangerous and protective. The reason being that the message will be the same on this side of the transfer if this MCU is using the same Encryption key. Though if there was a mistype of the key on either side would lead to an unreadable message, which is what the “Hacker” will get as they do not have to correct encryption key.

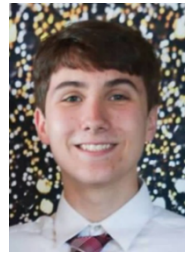
XI. Conclusion

The project required a multidisciplinary team able to integrate electronics, optics, and software in the same system for the intended purpose of transmitting information through optic fiber. The transmission of information through the optic fiber is the core of the project. However, it also requires electric components for its development into a complex multiplexing system that can multiplex the data transmission through switches that are controlled by an MCU, which requires developed software to define the switches combination for the multiplexing. Thus, this project shows the acquired skills over the years of studying disciplines such as electrical engineering, optics and photonics, and lastly, computer engineering at UCF so that they can be put into practice in a multidisciplinary team.

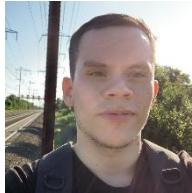
THE ENGINEERS



James Ko is a 22-year old graduating Computer Engineering student looking to apply to law school in the University of Colorado focusing on Cyber and Technology Law.



Justin Gruber is a 21-year old graduating Photonic Science and Engineering student and will be enrolling as a PhD student at the University of Rochester studying optics after graduation.



Edgar Nino is a 26-year old graduate of Electrical Engineering and will continue as a Master's student at the University of Central Florida.



Francisco Hernandez is a 22 year old graduating in Electrical Engineering and Photonic Science and Engineering. He currently interns at Lockheed Martin's RF Engineering Group under the CWEP program and plans to pursue a PhD in Photonics at CREOL after graduation.

References

- [1] Devgan, Preetpaul. “RF Photonic Applications (Preprint).” RF PHOTONIC APPLICATIONS (Preprint), Mar. 2021, apps.dtic.mil/sti/trecms/pdf/AD1124158.pdf.
- [2] Introduction to Waveplates, www.newport.com/n/introduction-to-waveplates. Accessed 4 Apr.
- [3] “What is AES Encryption and How Does It work?,” https://www.simplilearn.com/tutorials/cryptography-tutorial/aes-encryption
- [4] Keiser, G., Fiber Optic Communications. 2021, Singapore: Springer.
- [5] ITU. G.694.2 : Spectral grids for WDM applications: CWDM wavelength grid. 2003 [cited 2023 December 5]; Available from: <https://www.itu.int/rec/T-REC-G.694.2/en>
- [3] Hecht, E., Optics. 5th ed. 2016: Pearson Education, inc. 720.